LIP-STUDENTS-19-05

Measurement of J/ψ polarization in pp collisions at $\sqrt{s} = 8$ TeV in CMS

Francisco Albergaria[1,a] and Henrique Borges[1,b]

[1] *Instituto Superior Técnico, University of Lisbon*

Project supervisors: M. Araújo, P. Faccioli, J. Seixas

October 2010

Abstract.
The polarization of prompt J/ψ mesons is measured in proton-proton collisions at $\sqrt{s} = 8$ TeV, using a dimuon data sample collected by the CMS experiment at the LHC. The prompt polarization parameter λ_θ is measured from the dimuon decay angular distributions in the helicity frame. The J/ψ results are obtained in the transverse momentum range $12 < p_T < 70$ GeV and in the rapidity intervals $|y| < 1.5$.
No evidence of large polarization is seen in these kinematic regions, which is in agreement with past results using earlier data. Preliminary results of this analysis are shown here for the first time.

Keywords: Quarkonium, Polarization, NRQCD, QCD, Hadron formation

1 Introduction

Non-relativistic quantum chromodynamics (NRQCD) is the most satisfactory effective theory capable of explaining the production and decay of heavy quarkonium. However, the polarization of J/ψ mesons is not correctly described in this theory, where the purely perturbative colour-singlet production is complemented by processes including possible non-perturbative transitions from colour octet states to the observable bound states. Therefore, it is crucial to analyze the most recent experimental data, which already reaches rather high quarkonium transverse momentum, p_t, (where the calculations are expected to be more reliable [1]), and compare it with the theory predictions. In fact, for high transverse momentum, the directly produced S-wave quarkonia are expected to be transversely polarized with respect to the direction of their own momentum. If inconsistencies between the predictions made by the theory and the experimental results are found, it is important to discover if those discrepancies are originated from approximations and inaccuracies of the fixed-order perturbative calculations available at the moment or from difficulties in the conceptual basis of the theory.

Through the study of the angular distribution of the leptons produced in the $J^{PC} = 1^{--}$ quarkonium states' $\mu^+\mu^-$ decay, we can measure their polarization, determined by the lambda parameters, from the expression provided by Quantum Mechanics:

$$W(\cos\vartheta, \varphi) = \sum_{i=1}^{n} f^{(i)} W^{(i)} = \Big(1 + \lambda_\theta \cos^2\vartheta + \lambda_\varphi \sin^2\vartheta \cos 2\varphi + \lambda_{\varphi\vartheta} \sin 2\vartheta \cos\varphi\Big) \frac{3}{4\pi(3+\lambda_\theta)}, \quad (1)$$

with φ and ϑ being, respectively, the azimuthal and polar angles of the μ^+, with respect to the z axis of the selected polarization frame [2].

[a] e-mail: francisco.albergaria@tecnico.ulisboa.pt
[b] e-mail: henrique.joao.machado.borges@tecnico.ulisboa.pt

It is important to state that the majority of the theoretical studies on J/ψ polarization are limited to λ_θ, even though all the coefficients give independent information [3]. In this paper (as well), we only considered the $\cos(\theta)$ distribution. However, correct quarkonium polarization measurements require information from all the angular distribution parameters, in at least two polarization frames.

The definition of a coordinate system, with respect to which the momentum of one of the two decay products is expressed in spherical coordinates, is needed for the measurement of the distribution under study. In inclusive quarkonium measurements, the reference frame axes are fixed with respect to the physical reference provided by the directions of the two colliding beams as seen from the quarkonium rest frame. In this analysis, we considered the helicity frame, HX, that is the opposite of the direction of motion of the interaction point (i.e. the flight direction of the quarkonium itself in the center-of-mass of the colliding beams), as stated in [4]. A formal and intuitive description of the three most used definitions of the polarization axis z (decay reference frame) with respect to the directions of motion of the colliding beams and of the quarkonium can be found in the last reference cited.

In this analysis, we considered pp collision data obtained by the CMS experiment in 2012 at $\sqrt{s} = 8$ TeV with both J/ψ mesons in transverse momentum range $12 < p_T < 70$ GeV and in the rapidity intervals $|y| < 1.5$ and a Monte Carlo simulation generated assuming unpolarized production (uniform J/ψ decay distribution).

2 CMS detector and Data Processing

The CMS apparatus [5] was designed around a central element: a superconducting solenoid of 6 m internal diameter, providing a 3.8 T field. Within the solenoid volume are a silicon pixel and strip tracker, a lead tungstate crystal electromagnetic calorimeter, and a brass/scintillator hadron calorimeter. Muons are measured in gas-ionization detectors embedded in the steel return yoke outside the solenoid and made using three technologies: drift tubes,

cathode strip chambers, and resistive plate chambers. Extensive forward calorimetry complements the coverage provided by the barrel and end cap detectors. The main subdetectors used in this analysis are the silicon tracker and the muon system, which enable the measurement of muon momenta over the pseudorapidity range $|\eta| < 2.4$.

The events were collected using a two-level trigger system. The first level consists of custom hardware processors and uses information from the muon system to select events with two muons. The "high-level trigger" significantly reduces the number of events written to permanent storage by requiring an opposite-sign muon pair that fulfills certain kinematic conditions: invariant mass $2.8 < M < 3.35$ GeV, $p_T > 9.9$ GeV, and $|y| < 1.25$ for the J/ψ trigger. No p_T requirement is imposed on the single muons at trigger level, only on the dimuon. Both triggers require a dimuon vertex-fit χ^2 probability greater than 0.5%. Events where the two muons bend towards each other in the magnetic field are rejected to lower the trigger rate while retaining the events where the dimuon detection efficiencies are most reliable. The dimuons are reconstructed by combining two opposite-sign muons. The muon tracks are required to have hits in at least 11 tracker layers, at least two of which should be in the silicon pixel detector, and to be matched with at least one segment in the muon system. They must have a good track-fit quality (χ^2 per degree of freedom smaller than 1.8) and point to the interaction region. The selected muons must also be close, in pseudorapidity and azimuthal angle, to the muon objects responsible for triggering the event.

The single-muon detection efficiencies are measured by a tag-and-probe technique, using event samples collected with dedicated triggers enriched in dimuons from J/ψ decays, where a muon is combined with a track and the pair is required to have an invariant mass within the range 2.8 - 3.4 GeV. The measurement procedure has been validated in the fiducial region of the analysis with detailed Monte Carlo (MC) simulation studies. The single-muon efficiencies are precisely measured and parametrized as a function of p_T, in eight $|\eta|$ bins, to avoid biases in the angular distributions that could mimic polarization effects. Their uncertainties, reflecting the statistical precision of the tag-and-probe samples and possible imperfections of the parametrization, contribute to the systematic uncertainty in the polarization measurement. At high dimuon p_T, when the two decay muons might be emitted relatively close to each other, the dimuon trigger has a lower efficiency than the simple product of the two single-muon efficiencies. Detailed MC simulations, validated with data collected with single-muon and dimuon triggers, are used to correct these trigger-induced muon-pair correlations. A complete description of the CMS detector can be found in Ref. [5].

3 Event reconstruction and selection

It is of extreme importance to clean the sample, define the phase space, and reduce combinatorial background and contamination from nonprompt J/ψ. For that reason, the following kinematic and geometrical cuts on the muons and J/ψ mesons were applied in this analysis:

- Single muon $p_T > 6$ GeV;
- Single muon absolute pseudorapidity $|\eta| < 2.0$;
- Dimuon rapidity $|y| < 1.5$;
- J/ψ invariant mass in $[3, 3.2]$ GeV ;
- J/ψ $p_T \in [12, 70]$ GeV;
- Dimuon lifetime significance $|ct/ct_{err}| < 2$.

A total of 10528090 data events and 745530 events from the Monte Carlo simulation satisfy the above selection criteria.

4 Extraction of the polarization parameters

We divided the sample in 9 bins of dimuon p_T, determined so that the resulting uncertainty is comparable in all bins, obtaining (in GeV): [12, 14], [14, 15.5], [15.5, 17.5], [17.5, 19], [19, 21], [21, 22.5], [22.5, 25], [25, 29], [29, 70].

For each p_T bin the $\cos(\theta)$ distribution was obtained in the helicity frame both for the experimental and the MC simulation data. Figure 1 shows the experimental data $\cos(\theta)$ distribution for bin 1 and figure 2 shows the MC simulation data $\cos(\theta)$ distribution for bin 1. Comparing these distributions we can see that they are similar. In fact, the first one has a standard deviation of 0.1107 with an almost zero mean (the mean is actually equal to -1.059×10^4) and the second one has a standard deviation of 0.1106 with an almost zero mean (the mean is equal to -2.636×10^5). The width of the experimental peak is in agreement with what is expected from the MC simulation and the difference between means is negligible, which indicates consistency between both distributions. Observe that this has a profound physical meaning, Monte Carlo simulation was generated assuming unpolarized production (as mentioned in section 1), so this conformity between both distributions suggest that the J/ψ is produced unpolarized in experimental data too. It will be shown later that this hypothesis is confirmed by the results obtained in this analysis.

On the other hand, figure 3 shows the experimental data $\cos(\theta)$ distribution for bin 9 and it is possible to see that the range in $\cos(\theta)$ in this distribution is bigger than in the distributions for bin 1, as expected. However, in both cases, the number of events reaches its minimum for higher values of $|\cos(\theta)|$. This occurs because, for this situation, one muon (of the pair) has an insignificant momentum in the center-of-mass frame of the collision. As matter of fact, the range of values of $\cos(\theta)$ (that we can obtain) increases with p_T. For lower values of p_T, the accessible p_T for the muons will also be lower and, for values (of $\cos(\theta)$) that are distant from the mean of the distribution, it would be easier to achieve the situation where one muon has an small momentum in the center-of-mass frame of the collision (and, subsequently, the number of events would

be lower). For that reason, we have a bigger dispersion in our distribution for bins associated with high p_T.

For each bin, the quotient between experimental data and MC simulation data was determined in order to recover, in this way, the physical distribution. Note that shaping effects of acceptance and efficiency, affecting both data and MC, and also MC physical distribution being uniform means that dividing the data by MC is a way to correct the effects of acceptance and efficiency.

Observe that the integration over ϕ of the equation 1 leads to a function of the form $A(1 + \lambda \cos^2(\theta))$, that can be utilized for the determination of the parameter of the observed angular distribution (λ_θ). For that reason, this formula was fitted to the quotient distribution. The fitting procedure is carried out with no constraints applied to the fit parameters. These distributions and respective fits can be found in figures 4 to 12.

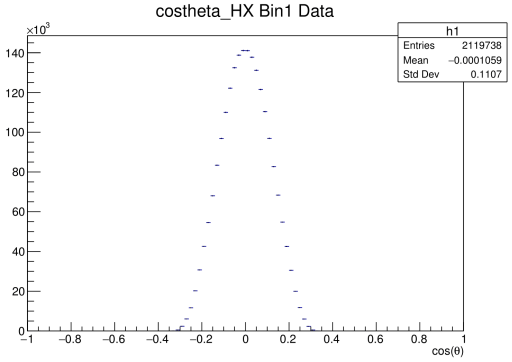

Figure 1. Experimental data cos(θ) distribution for bin 1.

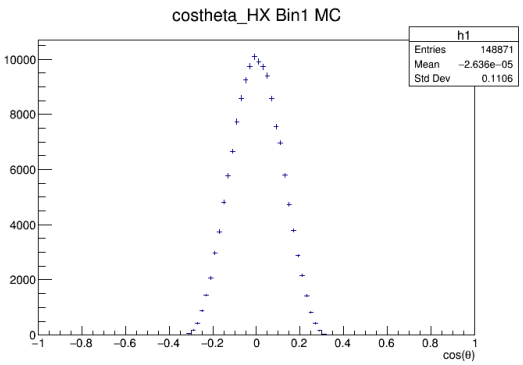

Figure 2. Monte Carlo data cos(θ) distribution for bin 1.

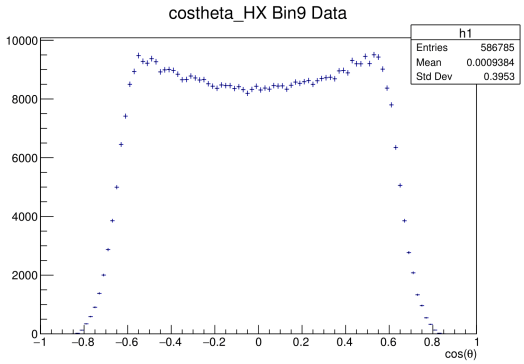

Figure 3. Experimental data cos(θ) distribution for bin 9.

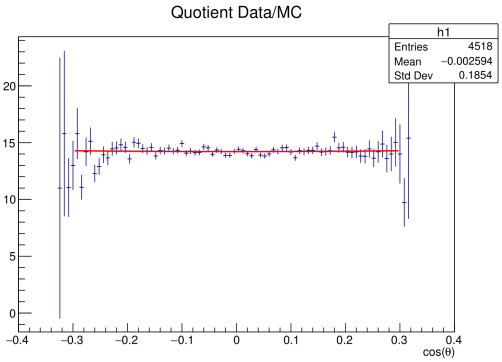

Figure 4. Bin 1: $\chi^2 = 82.9837$, $NDF = 72$

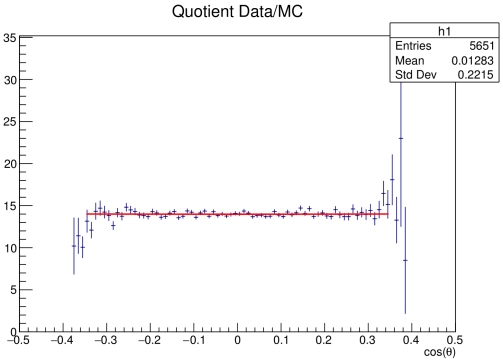

Figure 5. Bin 2: $\chi^2 = 67.9176$, $NDF = 68$

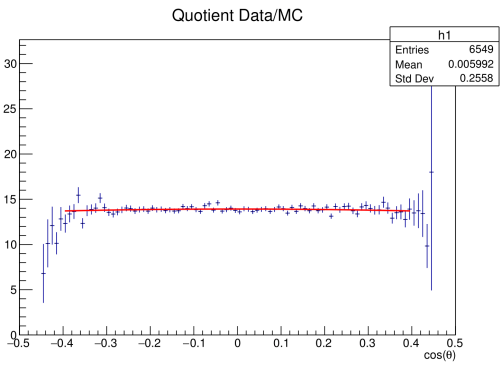

Figure 6. Bin 3: $\chi^2 = 70.1499$, $NDF = 78$

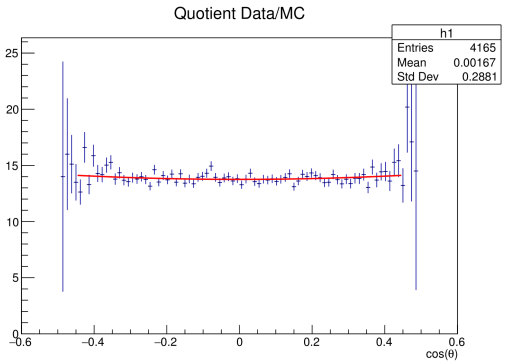

Figure 7. Bin 4: $\chi^2 = 70.7223$, $NDF = 73$

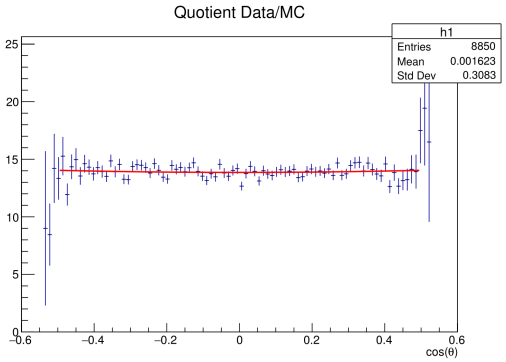

Figure 8. Bin 5: $\chi^2 = 89.957$, $NDF = 82$

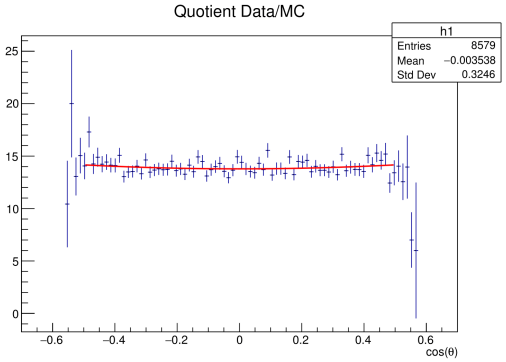

Figure 9. Bin 6: $\chi^2 = 65.6946$, $NDF = 70$

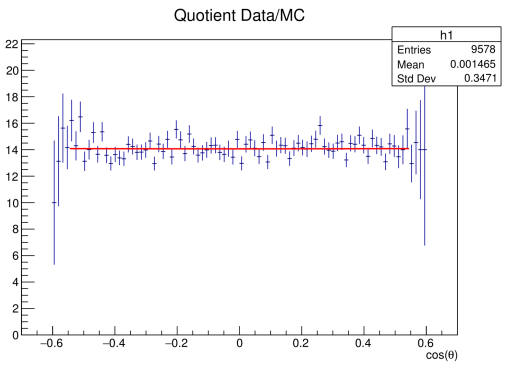

Figure 10. Bin 7: $\chi^2 = 83.3194$, $NDF = 76$

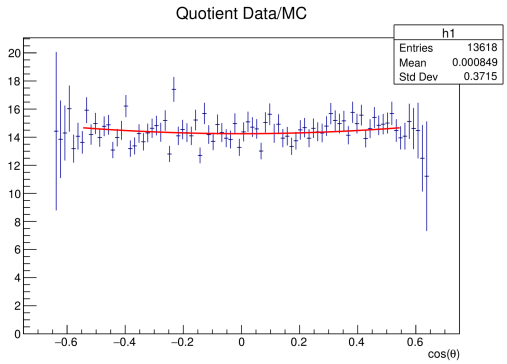

Figure 11. Bin 8: $\chi^2 = 100.439$, $NDF = 72$

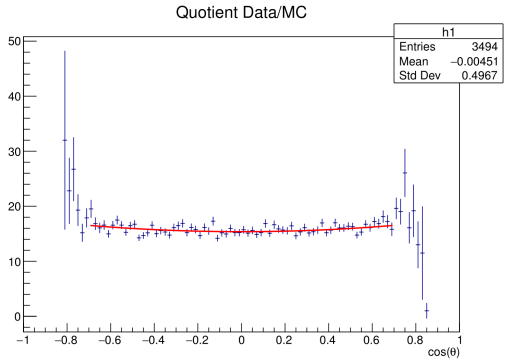

Figure 12. Bin 9: $\chi^2 = 81.7336$, $NDF = 68$

5 Results

With the parameters obtained from the fits, nine values of λ were obtained. A plot of λ as a function of the average p_T for experimental data on each bin can be found in figure 13.

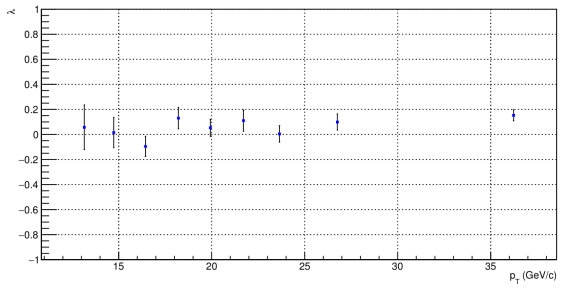

Figure 13. λ as a function of p_T.

6 Summary and conclusions

From figure 13 we can see that λ_θ is compatible with zero, which means that the J/ψ is produced almost unpolarized. This is in agreement with the previously published CMS result using earlier data presented in figure 14:

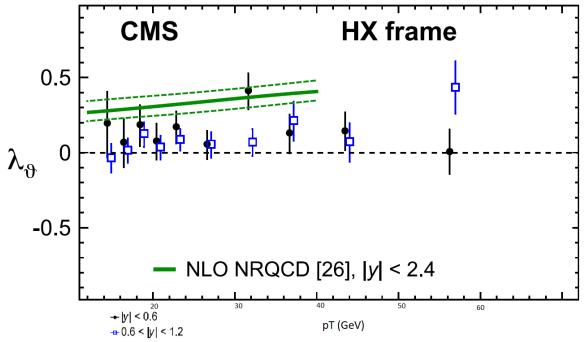

Figure 14. Polarization parameter λ_θ measured in the HX frame for prompt J/ψ, as a function of p_T and for several $|y|$ bins. The error bars represent total uncertainties (at 68.3% CL). The curve represent calculations of λ_θ from NLO NRQCD, with the dashed lines illustrating their uncertainties [2].

However, as the measurements exclude the hypothesis of a significant non-zero polarization, both results are in clear contradiction with NLO NRQCD.

In future analyses, it will be necessary to extend measurements to higher p_T where the theory is expected to be more reliable and the results more fruitful. It will also be important to determine systematic uncertainties, for example, by changing the selection cuts and the intervals in $\cos(\theta)$ used in the fits.

A more complete analysis requires the determination of the full decay distribution in two different reference frames, as stated in section 1, that will give us information for the variable $\widetilde{\lambda} = (\lambda_\vartheta, \lambda_\varphi, \lambda_{\vartheta\varphi})$. Furthermore, information on the direction of the spin-alignment of the decaying particle can be given through the latter parameters. The definition of $\widetilde{\lambda}$ and its experimental importance is explained in Ref. [4].

Acknowledgements

We gratefully acknowledge LIP (Laboratório de Instrumentação e Física Experimental de Partículas) for providing resources and support. We thank, in particular, the Quarkonia Group (Mariana Araújo, Pietro Faccioli and João Seixas) and, also, Carlos Lourenço for their guidance, help, insight and expertise that greatly assisted this internship.

References

[1] P. Faccioli, V. Knünz, C. Lourenço, J. Seixas, H.K. Wöhri, Physics Letters B **69**, 98 (2014)

[2] CMS Collaboration, Physics Letters B **727**, 381 (2013)

[3] Yu Feng and Bin Gong and Chao-Hsi Chang and Jian-Xiong Wang, Physical Review D **99** (2019)

[4] P. Faccioli, C. Lourenço, J. Seixas, H.K. Wöhri, The European Physical Journal C **69**, 657 (2010)

[5] CMS Collaboration, J. Instrum. **3**, S08004 (2008)